'Edgetic' perturbation of a *C. elegans* BCL2 ortholog

Matija Dreze[1,2,5], Benoit Charloteaux[1,3,5], Stuart Milstein[1,4,5], Pierre-Olivier Vidalain[1,4,5], Muhammed A Yildirim[1], Quan Zhong[1], Nenad Svrzikapa[1,4], Viviana Romero[1], Géraldine Laloux[1,2], Robert Brasseur[3], Jean Vandenhaute[2], Mike Boxem[1,4], Michael E Cusick[1], David E Hill[1] & Marc Vidal[1]

Genes and gene products do not function in isolation but within highly interconnected 'interactome' networks, modeled as graphs of nodes and edges representing macromolecules and interactions between them, respectively. We propose to investigate genotype-phenotype associations by methodical use of alleles that lack single interactions, while retaining all others, in contrast to genetic approaches designed to eliminate gene products completely. We describe an integrated strategy based on the reverse yeast two-hybrid system to isolate and characterize such edge-specific, or 'edgetic', alleles. We established a proof of concept with CED-9, a *Caenorhabditis elegans* BCL2 ortholog. Using *ced-9* edgetic alleles, we uncovered a new potential functional link between apoptosis and a centrosomal protein. This approach is amenable to higher throughput and is particularly applicable to interactome network analysis in organisms for which transgenesis is straightforward.

Classical 'forward' genetics and functional genomics or 'reverse' genetics have together assigned potential function(s) to tens of thousands of genes across dozens of organisms. With the availability of genome sequences and the development of automated phenotypic analyses, reverse genetics strategies based on null or nearly null alleles are rapidly becoming a major source of gene function information. However, functional interpretation of (nearly) null alleles is often complicated because gene products do not operate in isolation but act on each other within complex and dynamic interaction, or 'interactome', networks[1,2].

In interactome graphs, in which macromolecules and interactions between them are represented by 'nodes' and 'edges', respectively, knockouts or knockdowns should be modeled as eliminating a node and all its edges (**Fig. 1a**). More precise determination of molecular function(s) should occur with the development of new systematic strategies to generate alleles that perturb a single interaction, or edge at a time, while maintaining all others unperturbed. Systematic use of such 'edgetic' alleles should be useful to evaluate *in vivo* roles of individual interactions (**Fig. 1b**).

The reverse yeast two-hybrid (R-Y2H) and one-hybrid (R-Y1H) systems rely on genetic selections to identify mutations that disrupt protein-protein and DNA-protein interactions[3–6]. The efficiency of early R-Y2H versions was somewhat limited because most R-Y2H interaction-defective alleles correspond to truncation mutations unless a strategy is used to enrich for missense mutations[5,7–9]. Although dual-reporter systems had been developed to eliminate missense alleles, these systems only allow assaying two partners of a protein simultaneously and are limited if the two partners bind to the same region[10,11].

Here we describe an integrated strategy to systematically isolate edgetic alleles for subsequent *in vivo* characterization. We applied this strategy to *C. elegans* CED-9 (ref. 12), an ortholog of the human antiapoptotic oncoprotein BCL2. We efficiently identified edgetic alleles with various interaction defects caused by specific perturbations of CED-9 binding sites. A subset of *ced-9* edgetic alleles reintroduced *in vivo* caused phenotypes clearly distinct from the *ced-9* null phenotype, and suggestive of a physical and functional link between apoptosis and the centrosome. Our integrated pipeline interrogates interaction networks by perturbing edges instead of nodes and therefore complements the technological arsenal provided by gene knockouts and gene knockdowns to systematically investigate gene function.

RESULTS

Currently available *ced-9* alleles

CED-9 prevents apoptosis by sequestering the Apaf-1 ortholog CED-4 (ref. 13). Apoptosis is triggered when EGL-1 (a BCL2 homology domain 3 (BH3) protein) expression is turned on[14]. By physically interacting with CED-9, EGL-1 triggers conformational changes in CED-9, releasing CED-4 and allowing CED-4–mediated activation of the CED-3 caspase[15,16].

The *ced-9* gene was initially identified through the isolation of a dominant allele, *ced-9(n1950)*, which suppresses apoptosis[12,17]. In this allele, a single amino acid change (G169E) in the encoded protein prevents EGL-1–induced dissociation of otherwise wild-type CED-9/CED-4 complex formation, and thus CED-9(G169E)

[1]Center for Cancer Systems Biology (CCSB) and Department of Cancer Biology, Dana-Farber Cancer Institute, and Department of Genetics, Harvard Medical School, Boston, Massachusetts, USA. [2]Unité de Recherche en Biologie Moléculaire, Facultés Universitaires Notre-Dame de la Paix, Namur, Wallonia, Belgium. [3]Centre de Biophysique Moléculaire Numérique, Faculté Universitaire des Sciences Agronomiques de Gembloux, Gembloux, Wallonia, Belgium. [4]Present addresses: Alnylam Pharmaceuticals, Cambridge, Massachusetts, USA (S.M. and N.S.), Laboratoire de Génomique Virale et Vaccination, Centre National de la Recherche Scientifique, Unité de Recherche Associée 3015, Institut Pasteur, Paris, France (P.-O.V.) and Utrecht University, Utrecht, The Netherlands (M.B.). [5]These authors contributed equally to this work. Correspondence should be addressed to M.V. (marc_vidal@dfci.harvard.edu).

RECEIVED 6 APRIL; ACCEPTED 28 SEPTEMBER; PUBLISHED ONLINE 25 OCTOBER 2009; CORRECTED ONLINE 16 NOVEMBER 2009; DOI:10.1038/NMETH.1394

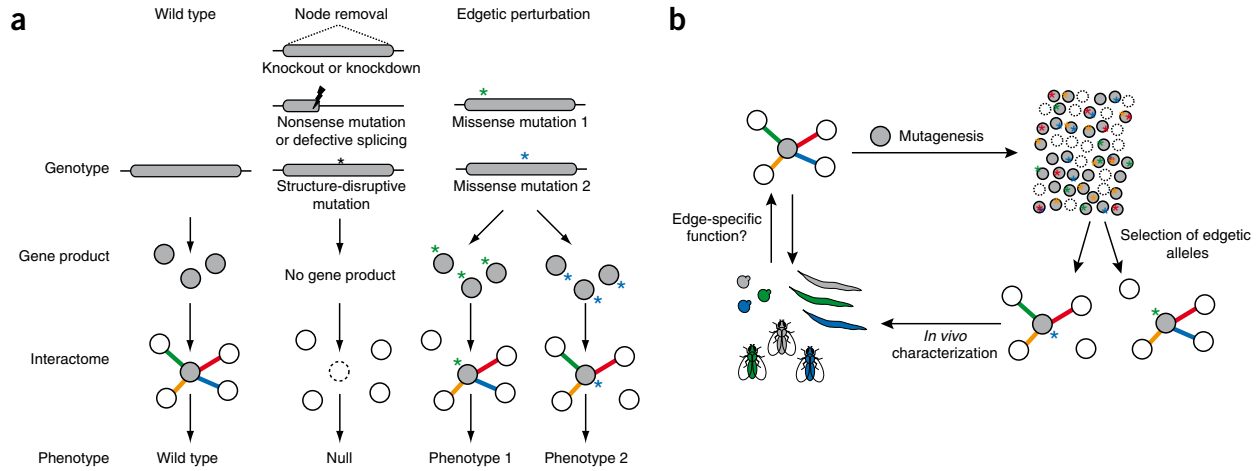

Figure 1 | Schematic representations of genotype-phenotype associations. (**a**) Possible phenotypes resulting from distinct network perturbations caused by different experimental strategies or mutation types. (**b**) Edgetic strategy applied to a protein of interest (gray node). Colors represent specific edges, their specific perturbation and the specific corresponding phenotypes. Dashed circles represent absent, truncated or unstable gene products.

can be considered edgetic by our definition. All four additional alleles currently available (*ced-9*(*n2812*), *ced-9*(*n2077*), *ced-9*(*n2161*) and *ced-9*(*n1653*ts)) result in complete or near complete CED-9 depletion, that is, CED-9 node removal (**Supplementary Fig. 1**).

Isolation of *ced-9* edgetic alleles

We tested whether our strategy could be used to isolate alleles encoding CED-9(G169E)-like proteins. We first determined that Y2H is suitable to (i) detect the CED-9/CED-4 interaction, (ii) reconstitute the EGL-1–induced dissociation of this interaction and (iii) recapitulate the CED-9(G169E) edgetic profile (**Fig. 2a**,**b** and **Supplementary Data 1**). We then developed a Y2H-based scheme starting from a library of random *ced-9* mutations produced by PCR amplification of a truncated *ced-9* gene, encoding CED-9 lacking its C-terminal transmembrane domain (CED-9ΔTM). The library was enriched for full-length open reading frames (ORFs) (**Fig. 2c** and **Supplementary Table 1**). From this library, we selected for alleles encoding CED-9(G169E)–like proteins based

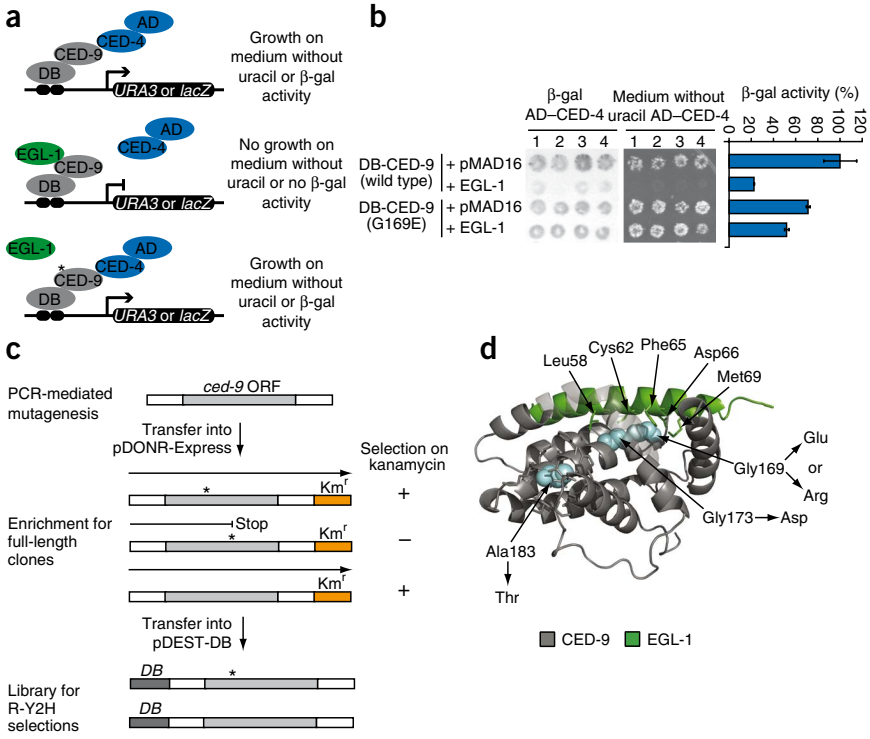

Figure 2 | Isolation of *ced-9* alleles insensitive to EGL-1. (**a**) Schematic of a modified Y2H assay used to identify edgetic alleles that maintain CED-9 interaction with CED-4 in presence of EGL-1. DB, Gal4 DNA-binding domain. AD, Gal4 activation domain. β-gal, β-galactosidase. (**b**) Y2H phenotypes of the interaction between AD–CED-4 and DB–CED-9 (wild type or G169E) in the absence or presence of EGL-1. Each assay was performed in quadruplicate (1–4): filter β-galactosidase assay (β-gal; left), growth assay on medium without uracil (middle) and a quantitative β-galactosidase assay (β-gal activity; right). Error bars, s.e.m. ($n = 4$). (**c**) To generate the CED-9ΔTM mutant library, ORFs mutagenized by PCR were cloned by Gateway reaction into pDONR-Express, a bacterial expression vector containing a kanamycin resistance–encoding gene (Km^r) placed in-frame with the ORF cloning site[8]. The selection of *Escherichia coli* transformants on kanamycin-containing plates was designed to eliminate nonsense mutations and out-of-frame changes, enriching the library with full-length ORFs that can then be transferred into the pDEST-DB Y2H vector by Gateway reaction for R-Y2H selections. White boxes surrounding *ced-9* ORF represent Gateway recombination sites. (**d**) Crystal structure of a CED-9/EGL-1 complex (Protein Data Bank (PDB) identifier: 1TY4)[18] with residues mutated in proteins encoded by *ced-9* edgetic alleles indicated in blue. Substitutions are indicated. EGL-1 residues less than 4 Å away from CED-9 mutated residues and CED-9 residues less than 4 Å away from A183 are shown as sticks. For clarity hydrogen atoms have been omitted.

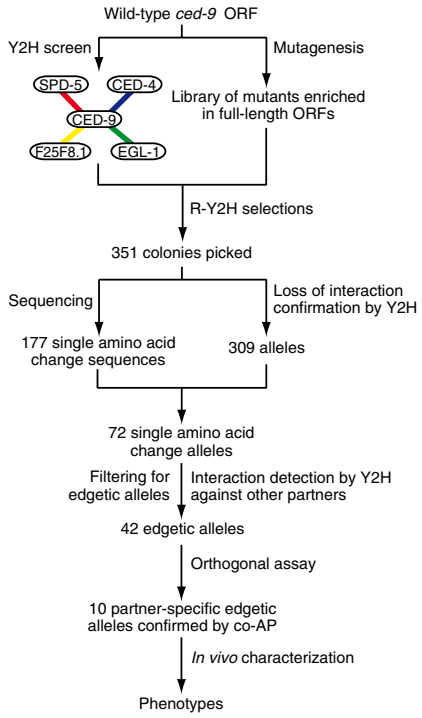

Figure 3 | Outline of the edgetic strategy. The interaction network of CED-9 was mapped by Y2H and confirmed by co-AP. In parallel, a CED-9ΔTM mutant library enriched for full-length ORFs was generated. Interaction-defective alleles were isolated by R-Y2H from the CED-9ΔTM mutant library. *ced-9* alleles PCR-amplified directly from yeast colonies were sequenced to identify potential mutations, and then reintroduced by gap repair into fresh yeast cells to confirm loss-of-interaction phenotypes by Y2H. Interaction-defective alleles were subsequently tested by Y2H against other CED-9 partners to distinguish between edgetic and non-edgetic alleles. The interaction profiles of a subset of partner-specific edgetic alleles were validated by co-AP. Validated alleles were expressed *in vivo*, and phenotypic consequences were examined.

on their ability to maintain the interaction with CED-4 in the presence of EGL-1, thus conferring growth on selective medium lacking uracil (**Fig. 2a**).

We identified four such alleles. Two of these alleles encoded proteins with substitutions of Gly169, the amino acid mutated in the protein encoded by *ced-9(1950)*, the dominant allele originally isolated in a forward genetic screen (**Fig. 2d**). One change corresponded exactly to the previously described *ced-9(1950)* G169E substitution, demonstrating the power of our Y2H genetic selection. The other change, G169R, was new but similar to G169E (substitution of a glycine by a bulky charged residue). The third allele encoded a protein with a G173D mutation, a substitution of a glycine close to Gly169 in the CED-9 sequence. In the CED-9/EGL-1 co-crystal[18], Gly169 and Gly173 are adjacent and are both in contact with the EGL-1 BH3 peptide (**Fig. 2d**). The A183T substitution in the protein encoded by the fourth allele affects a residue outside of the EGL-1 BH3 binding groove but in the same α-helix as Gly169 and Gly173. An A183Y substitution decreases the melting temperature of the CED-9/EGL-1 complex by 5 °C (ref. 19), consistent with our observation that the A183T mutation affects the CED-9/EGL-1 interaction. Altogether we found that a genetic selection in the appropriate yeast strain background can efficiently isolate *ced-9* edgetic alleles.

Integrated strategy to isolate edgetic alleles

We generalized the approach for new interactions (**Fig. 3**). We screened CED-9ΔTM against *C. elegans* cDNA[20] and ORFeome[21] libraries by Y2H. We recovered both EGL-1 and CED-4 as CED-9ΔTM interactors, validating our Y2H screen[14,22]. We also identified two new Y2H interactors: residues 829–1,198 of SPD-5 and full-length F25F8.1. SPD-5 is a centriole protein essential for centrosome maturation and mitotic spindle assembly[23]. F25F8.1 is an uncharacterized protein with no known orthologs outside of the *Caenorhabditis* genus. We validated all Y2H interactions by co-affinity purification (co-AP) in HEK293T cells using glutathione S-transferase (GST) pulldown[21] with CED-9ΔTM and full-length EGL-1, CED-4, SPD-5 and F25F8.1 (**Supplementary Fig. 2**). Having validated SPD-5 and F25F8.1 as likely bona fide biophysical interactors, we used our edgetic strategy to interrogate the biological relevance of these interactions.

From the CED-9ΔTM mutant library (**Figs. 2c** and **3**), we used R-Y2H to select mutants unable to interact with either CED-4 or SPD-5, using *SPAL10::URA3* (ref. 6), a counterselectable marker that causes toxicity in the presence of 5-fluoroorotic acid (5-FOA)[24]; loss of interaction results in the ability to grow on plates containing 5-FOA. As the CED-9/F25F8.1 interaction does not confer 5-FOA sensitivity, we screened for *ced-9* mutants unable to interact with F25F8.1 by looking for decreased *GAL1::lacZ*–induced β-galactosidase activity (**Supplementary Data 2**). We obtained a total of 351 potential *ced-9* alleles, with 192, 144 and 15 of their gene products unable to interact with CED-4, SPD-5 and F25F8.1, respectively.

After PCR amplification of these potential alleles, we sequenced them and analyzed interactions by Y2H against all CED-9 partners to confirm the interaction defects and determine their specificity (**Fig. 3**, **Supplementary Figs. 3–5**, **Supplementary Tables 2–5** and **Supplementary Data 2**). We found 42 alleles with an edgetic profile (that is, disrupting one or a subset of interactions), each affecting one of 33 different amino acids along the CED-9 sequence (~13% of the sequence; **Supplementary Table 5**). In contrast, 30 alleles impaired all CED-9 binding capacities, and we therefore considered them non-edgetic.

We used co-AP pulldowns in HEK293T cells as an orthogonal protein-interaction assay[21,25]. We tested 16 partner-specific edgetic alleles encoding proteins defective in their ability to interact with CED-4 (five alleles), SPD-5 (nine alleles) or F25F8.1 (two alleles). We validated a substantial proportion of R-Y2H edgetic alleles (10/16) by co-AP (**Supplementary Fig. 6** and **Supplementary Data 2**).

Structural analysis of edgetic and non-edgetic residues

Although our edgetic strategy does not require a priori knowledge of tertiary structure, we could use such information to investigate the properties of residues mutated in edgetic and non-edgetic alleles ('edgetic' and 'non-edgetic' residues, respectively). To assess whether affected residues were preferentially located in protein-binding sites, we quantified their surface exposure in the CED-9 tertiary structure (**Fig. 4a**). We defined as solvent-accessible the residues with 10% or more of solvent-accessible surface area in at least one of the three available CED-9 crystal structures[16,18,19],

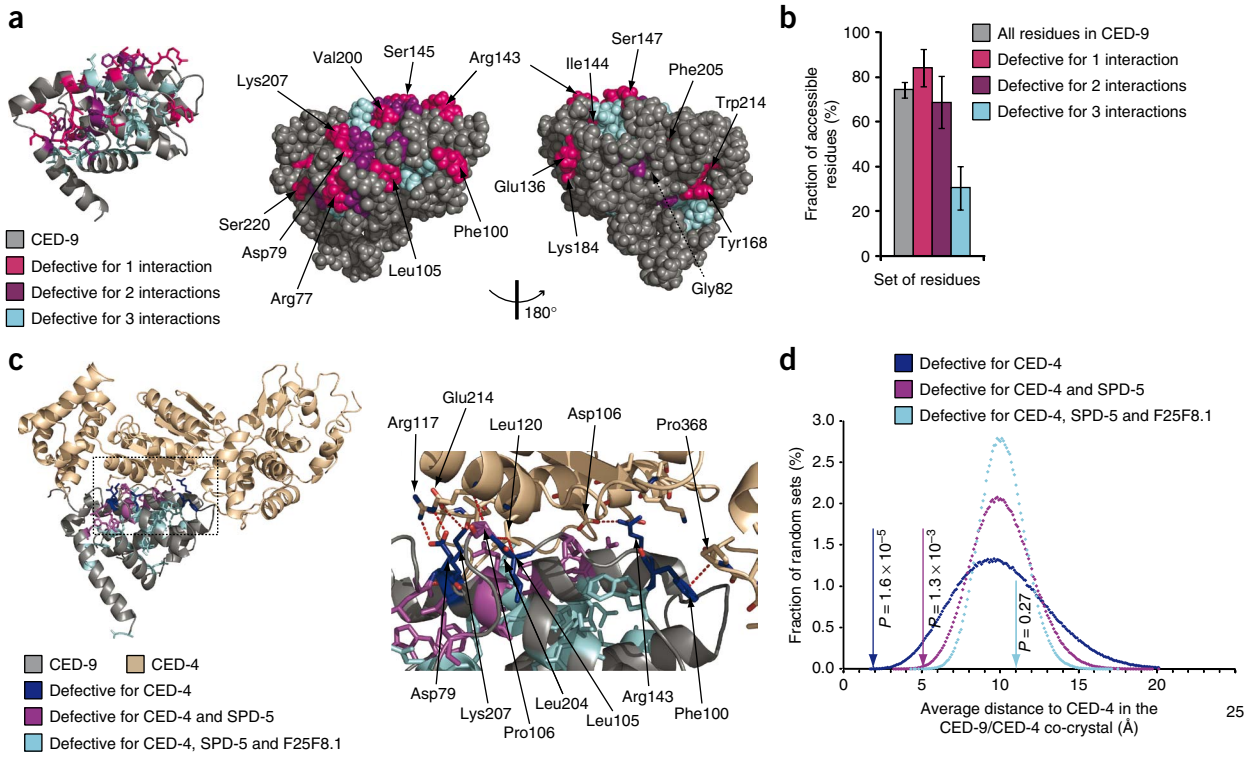

Figure 4 | Edgetic and non-edgetic residues in CED-9 and CED-9/CED-4 structures. (**a**) Ribbon diagram of CED-9 (PDB: 1OHU)[19] (left); residues mutated in R-Y2H alleles are shown as sticks (hydrogen atoms omitted). Space-filling representation of the same structure in the identical (middle) and opposite (right) orientations. Residues mutated in alleles defective for only one interaction are labeled. Gly82 (dashed line) is buried. (**b**) Fraction of residues (all residues versus the residues mutated in the indicated sets of *ced-9* alleles) accessible in at least one of the three CED-9 structures[16,18,19] using a 10% solvent-accessible surface area cutoff. Error bars, standard error for a binomial distribution. (**c**) Ribbon diagram of CED-9 complexed with one CED-4 monomer (PDB: 2A5Y)[16] (left); residues mutated in CED-4 interaction–defective alleles are shown as sticks. In the close-up of the same view (right), CED-4 residues that interact with CED-9 residues mutated in CED-4-specific edgetic alleles are also shown as sticks. Red dashed lines, interactions. Oxygen atoms are red and nitrogen atoms blue. Hydrogen atoms are omitted. (**d**) Distribution of the average distance to CED-4 in the CED-9/CED-4 co-crystal obtained for 1,000,000 random sets of 6, 14 or 24 residues as compared to the average distance (arrows) of the residues mutated in the indicated sets of CED-4 interaction–defective alleles.

taking into account variations between these structures. Edgetic residues, especially those mutated in proteins defective for one interaction, were on average more accessible than non-edgetic residues (**Fig. 4a**,**b** and **Supplementary Data 3**). The average surface exposure we observed for non-edgetic residues was significantly lower than expected by chance ($P < 10^{-6}$; empirical *P*-value; **Supplementary Fig. 7**).

These observations suggest that edgetic alleles of *ced-9* targeted relatively more accessible residues that are likely part of interaction regions. In contrast, non-edgetic alleles were defective for all three CED-9 interactions because of disruptive substitutions in the CED-9 core. The non-conservative nature of these substitutions corroborated this explanation (**Supplementary Table 5**). For instance, ten non-edgetic alleles (~1/3) encoded a protein with an α-helix residue mutated to proline. Notably, two non-edgetic alleles that we isolated contained a substitution of Y149, which is mutated in the protein encoded by the *ced-9*(*n1653*ts) allele (**Supplementary Fig. 1**) and is crucial for CED-9 structure[18]. This finding supports the proposal that non-edgetic alleles are defective for all interactions because of a disrupted CED-9 tertiary structure.

If non-edgetic mutations disrupt CED-9 tertiary structure and edgetic mutations affect specific interaction regions, non-edgetic alleles should tend to encode relatively unstable proteins. We expressed wild-type CED-9 as well as proteins encoded by 14 edgetic alleles and 14 non-edgetic alleles, all as GST fusion proteins in human cells (**Supplementary Fig. 8**). Proteins encoded by edgetic alleles were expressed at levels comparable to that of wild-type CED-9 fusion protein. In contrast, the non-edgetic mutant proteins could not be detected or were expressed at much lower levels than wild-type CED-9. As expected, two CED-9 truncated proteins also had reduced expression (Stop1 and Stop2; **Supplementary Fig. 8**). Non-edgetic mutations in Tyr149 (Y149C and Y149H) resulted in decreased stability and poor expression of CED-9 as previously reported for the Y149N mutant[18]. These data strongly suggest that edgetic and non-edgetic alleles result from distinct molecular defects: destabilization and degradation for the non-edgetic alleles and more subtle changes that do not affect overall stability for edgetic alleles.

Edgetic and non-edgetic residues in binding sites

To test our model for the structural basis of edgetic versus non-edgetic alleles, we took advantage of the CED-9/CED4 co-crystal[16], locating in this quaternary structure the residues mutated in all alleles defective for CED-4 interaction (**Fig. 4c**). All six distinct residues mutated in the alleles defective only for the CED-4 interaction were located at the CED-9/CED-4 interface,

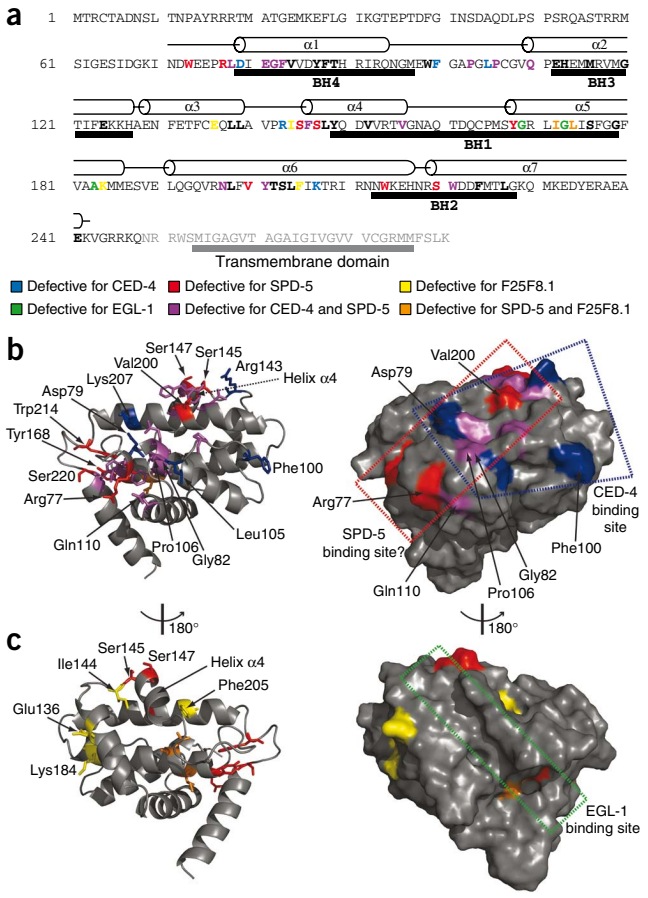

Figure 5 | Positioning edgetic residues in CED-9 structures. (**a**) Positions of edgetic residues in the CED-9 sequence. The portion of CED-9 present in the crystal (PDB: 1OHU)[19] and the α-helices observed in the corresponding structure are indicated above the sequence; BCL2 homology (BH) domains[19] are indicated under the sequence. Edgetic and non-edgetic residues are in bold font, edgetic residues are colored as indicated. (**b**) Ribbon diagram of the CED-9 structure (PDB: 2A5Y)[16] (left); residues mutated in edgetic alleles defective for CED-4 and/or SPD-5 interaction are shown as sticks. Helix α4 (the region undergoing EGL-1–induced conformational changes) is indicated[18]. Van der Waals surface of the same structure in identical orientation (right). The CED-4–binding site and the hypothetical SPD-5–binding site are shown. (**c**) Ribbon diagram of the CED-9 structure (PDB: 2A5Y)[16] (left) at opposite orientation with respect to **b**. Residues mutated in edgetic alleles defective for SPD-5 and/or F25F8.1 interactions are shown as sticks. Van der Waals surface of the same structure in identical orientation (right). The EGL-1 binding site is shown.

significantly more than expected by chance ($P = 1.2 \times 10^{-4}$; hypergeometric test). Half of the 14 residues mutated in the proteins encoded by edgetic alleles defective for CED-4 and one additional partner were at the CED-4 binding site, also more than expected by chance ($P = 0.022$; hypergeometric test). In contrast, only one of the 24 non-edgetic residues was in contact with CED-4, a significantly unlikely occurrence ($P = 9.5 \times 10^{-3}$; hypergeometric test).

We also compared the average distance to CED-4 of the residues in each set to the average distance of random sets of residues (**Fig. 4d**). Whereas 24 CED-9 residues picked at random had one chance in four to be further away from CED-4 than the non-edgetic residues ($P = 0.27$; empirical P-value), the edgetic residues were significantly closer to CED-4 than expected by chance ($P = 1.3 \times 10^{-3}$ and 1.6×10^{-5} for alleles defective for two and one interaction, respectively; empirical P-values). These results argue that mutations of edgetic residues likely result in the alteration of the CED-9/CED-4 interface, whereas mutations of non-edgetic residues likely disrupt the CED-9/CED-4 interaction by altering CED-9 structure.

As there is no obvious clustering of edgetic residues for any CED-9 interactor on the CED-9 primary sequence (**Fig. 5a**), suggesting that the binding sites for SPD-5, F25F8.1 and CED-4 are conformational, we used sets of edgetic residues to map the putative binding sites for SPD-5 and F25F8.1 (**Fig. 5b**,**c**, **Supplementary Figs. 9**,**10** and **Supplementary Data 4**). Our edgetic strategy enabled the isolation of partner-specific edgetic alleles for each CED-9 partner even though the CED-9 interaction surfaces seem intricate, with partly overlapping sites.

Node removal and edgetic perturbation *in vivo*

RNAi of *ced-9* (*ced-9*(RNAi)) in worms results in apoptosis-triggered embryonic lethality[26] because of increased germ-cell death (**Fig. 6a**). In addition to previously described defects in mitotic spindle assembly resulting in embryonic lethality[23], RNAi of *spd-5* also increased apoptosis in the germline, approximately half as much as *ced-9*(RNAi) (**Fig. 6a**). This is consistent with our identification of SPD-5 as a biophysical interactor of CED-9 and suggests that SPD-5, in addition to its role in mitosis, is also involved in apoptosis regulation. As with *ced-9*(RNAi), *spd-5*(RNAi)–induced germ-cell apoptosis was suppressed in a *ced-3* null background.

To evaluate whether the CED-9/SPD-5 interaction directly contributes to the embryonic lethality and germ-cell death observed upon *spd-5*(RNAi), we characterized worms carrying CED-9(W214R), a SPD-5–specific edgetic allele. In parallel, we analyzed worms carrying CED-9(K207E), a CED-4–specific edgetic allele, to evaluate the phenotypic consequences of perturbing the CED-9/CED-4 interaction.

We generated transgenic lines carrying genes encoding CED-9(K207E) and CED-9(W214R) by microparticle bombardment and crossed them into worms carrying the *ced-9*(*n2161*) null allele. Compared to worms rescued with a wild-type *ced-9* transgene, worms expressing CED-9(K207E) laid fewer embryos ($P = 0.04$; Student t-test), similar to *ced-9* null mutants (**Fig. 6b**). However wild-type *ced-9* transgene and both edgetic alleles rescued the embryonic lethality conferred by the *ced-9* null allele (**Fig. 6c**). Even though we cannot exclude that CED-9(K207E) could retain some residual capacity to bind CED-4 *in vivo*, the rescue observed with this transgene suggests that the antiapoptotic action of CED-9 during embryonic development is not exclusively correlated to CED-4 sequestration. These data also show that the embryonic lethality that occurs in worms subjected to *spd-5*(RNAi) is not necessarily due to loss of the CED-9/SPD-5 interaction as worms expressing CED-9(W214R) are viable.

The viability of transgenic worms expressing CED-9(K207E) or CED-9(W214R) allowed investigation of the role of CED-9/CED-4 and CED-9/SPD-5 interactions in germline apoptosis. We subjected worms to apoptotic challenges induced by *ced-4* (RNAi) and *cpb-3*(RNAi), which suppress and mildly increase germ-cell apoptosis, respectively[27,28]. Without an apoptotic challenge (*gfp*(RNAi)), worms expressing CED-9(K207E) and

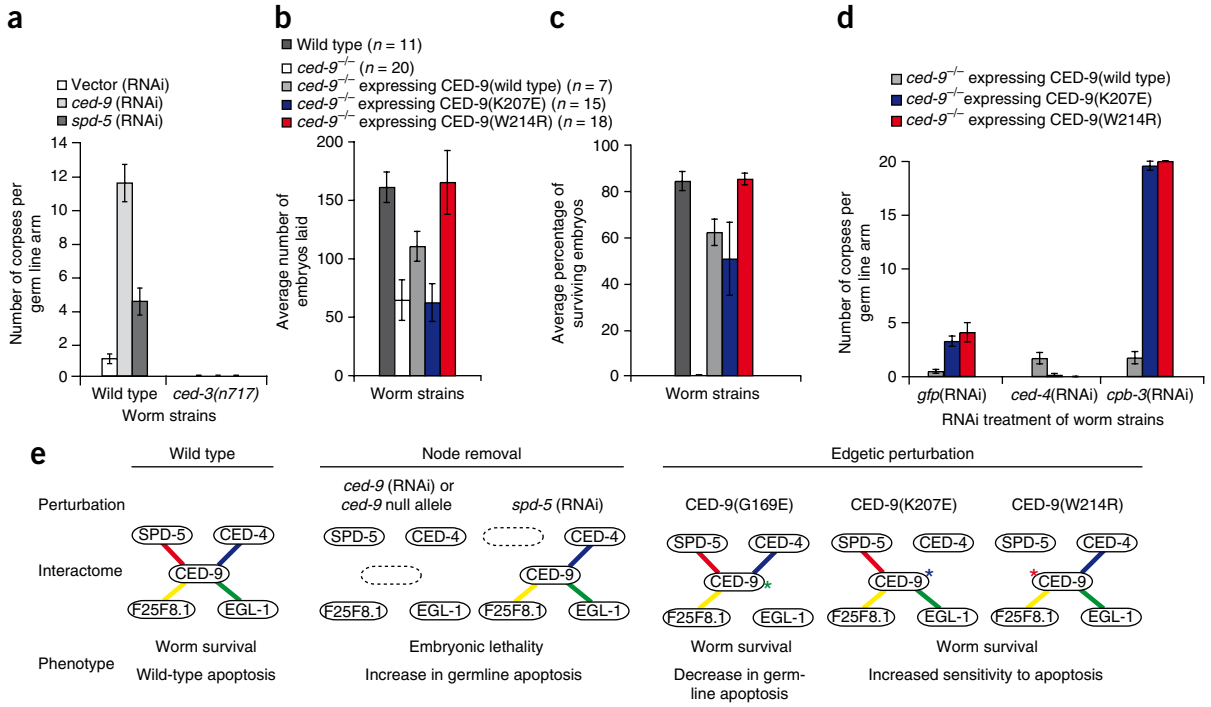

Figure 6 | Node removal and edgetic perturbation *in vivo*. (**a**) Corpse count per germline arm in wild-type (N2) or apoptosis-defective *ced-3(n717)* worms subjected to RNAi. Vector(RNAi) is the negative control. Errors bars, s.e.m. ($n = 15$). (**b**,**c**) Average number of embryos laid (**b**; error bars, s.e.m.) and fraction of worm broods reaching adulthood (**c**; error bars, s.e. for a binomial distribution) in the indicated strains. (**d**) Corpse count per germline arm in the indicated strains treated with RNAi targeting *gfp* (negative control), *ced-4* or *cpb-3*. Error bars, s.e.m. ($n = 12$, except for *gfp*(RNAi) and *cpb-3*(RNAi) of *ced-9*$^{-/-}$ expressing CED-9(wild-type) where $n = 9$ and 7, respectively). (**e**) Schematic of phenotypic consequences of selected network perturbations. Node removal is induced either by *ced-9* or *spd-5*(RNAi), while edgetic perturbation is caused by the CED-9(G169E)[12,17], CED-9(W214R) or CED-9(K207E) mutations. Wild-type, (*unc-69(e587)*) worm strain. *ced-9*$^{-/-}$: worm strain carrying a *ced-9* null allele (*ced-9*(*n1950n2161*)). CED-9 wild-type, CED-9(K207E) and CED-9(W214R) are expressed from constructs integrated into the *ced-9* null allele worm strain genetic background.

CED-9(W214R) exhibited a small increase in germline apoptosis compared to worms rescued with a wild-type *ced-9* allele (3.25, 4.08 and 0.44 dead cells, respectively, $P = 8.2 \times 10^{-5}$ and 0.05; Student *t*-test) (**Fig. 6d**), but germ-cell apoptosis in these worms was much less pronounced relative to *ced-9*(RNAi)–induced apoptosis (**Fig. 6a**). As anticipated, *ced-4*(RNAi) of CED-9(K207E) and CED-9(W214R) mutants suppressed apoptosis in the germline. RNAi treatment of *cpb-3* strongly increased germ-cell apoptosis in worms expressing CED-9(K207E) and CED-9(W214R), compared to the small increase observed in worms rescued with a wild-type *ced-9* allele (19.5, 20 and 1.72 dead cells, respectively, $P = 5.2 \times 10^{-12}$ and 5.8×10^{-8}; Student *t*-test). This finding suggests that, similarly to CED-9/CED-4, the CED-9/SPD-5 interaction also protects germ cells from apoptosis.

Node and edge removal can result in diverse phenotypic profiles, uncovering different aspects of the apoptosis module (**Fig. 6e**). The RNAi experiments we presented implicate *ced-9* and *spd-5* in *ced-3*–mediated germline apoptosis and reveal genetic links between these actors. As both *ced-9* and *spd-5* are essential genes, knockdowns lead to embryonic lethality, precluding characterization. Partner-specific edgetic alleles, which restore viability of mutant worms, underscore that in contrast to the CED-9/EGL-1 interaction, both CED-9/CED-4 and CED-9/SPD-5 protein-protein interactions contribute to negative control of germline apoptosis, especially in response to particular apoptotic triggers.

DISCUSSION

We present a strategy to select edgetic alleles defective for one or a few protein interactions, as a way to better understand their role in complex interaction networks. Applying this strategy to CED-9, we identified edgetic alleles whose gene products (i) lacked only a subset of interactions, (ii) had interaction defects that were likely due to specific changes in or close to protein interaction sites and (iii) had *in vivo* phenotypes different from those caused by null or near-null perturbations. An edgetic mutation that only affected the interaction between CED-9 and SPD-5 resulted in increased sensitivity to apoptotic stimuli. In contrast, the null phenotype for these genes was embryonic lethality. Hence, our platform is one alternative to define functions for essential genes beyond their null phenotype.

Though the biological function of the CED-9/SPD-5 interaction was not fully defined, there are two likely possibilities. The CED-9/SPD-5 interaction may be required to suppress apoptosis during spindle assembly, during centrosome assembly or at other times during cell division when SPD-5 is present. Alternatively SPD-5 may 'moonlight'[29] in the apoptotic pathway, given that loss of the CED-9/SPD-5 interaction sensitizes cells to apoptosis caused by loss of CPB-3, an RNA-binding protein with no known function in spindle assembly or cell division.

Biological systems consist of interaction networks in which many types of macromolecules associate with and act on each other, and biological properties of living organisms reflect the local and global properties of these networks. Several well-characterized

inherited human disease alleles associated with particular disease phenotypes have been shown to correspond to edgetic perturbations[30]. Among the many biophysical interactions identified so far, a critical step is to identify the biologically relevant ones[31] and understand how they contribute to cellular systems. To address such questions, tools that probe interactions (edges) are needed. Considering that tens of thousands of interactions have been mapped for an increasing number of organisms, such edgetic perturbation strategies must be compatible with high-throughput settings. Our platform is a reverse genetics strategy to interrogate protein-protein interactions in the context of interactome networks. We propose the systematic use of 'edgetic perturbation' reagents, whether as alleles or small compounds, to analyze the properties of interaction networks.

METHODS

Methods and any associated references are available in the online version of the paper at http://www.nature.com/naturemethods/.

Note: Supplementary information is available on the Nature Methods website.

ACKNOWLEDGMENTS

This paper is dedicated to the memory of Stan Korsmeyer. We thank the members of the Vidal Lab and of the Dana-Farber Cancer Institute CCSB and particularly A.-R. Carvunis for helpful discussions. This work was supported by US National Institutes of Health (NIH) grants R01 HG001715 from the National Human Genomics Research Institute (NHGRI) and National Institute of General Medical Sciences (NIGMS) and grants R33 CA105405, R33 CA132073 and R21/R33 CA081658 from the US National Cancer Institute (NCI) (M.V.), U01 CA105423 from the NCI (principal investigator, S. Orkin; project leader, M.V.) and by Institute Sponsored Research funds from the Dana-Farber Cancer Institute Strategic Initiative awarded to CCSB. M.D. and G.L. were supported by a 'Research Fellow' fellowship from the Fonds de la Recherche Scientifique (FRS-FNRS, French Community of Belgium). B.C. was supported by the Belgian Program on Interuniversity Attraction Poles initiated by the Federal Office for Scientific, Technical and Cultural Affairs (IAP P6/19 PROFUSA). S.M. was supported by an NIH National Research Service Award training grant fellowship (T32CA09361). P.-O.V. was supported by a European Molecular Biology Organization long-term fellowship 61-2002. Support was provided by the Leukemia Research Foundation to M.B. M.V. and R.B. thank the 'Fonds de la Recherche Scientifique (FRS-FNRS, French Community of Belgium)'. The content is solely the responsibility of the authors and does not necessarily represent the official views of the NCI, NHGRI, NIGMS or the NIH.

AUTHOR CONTRIBUTIONS

M.D., B.C., S.M., P.-O.V., M.A.Y., Q.Z., R.B., J.V., M.B. and M.V. conceived the experiments and analyses. S.M. and P.-O.V. generated the *ced-9* mutant library and performed Y2H screens and R-Y2H selections. M.D. and P.-O.V. cloned the alleles. P.-O.V. and M.D. performed the co-APs. M.D. and G.L. developed and implemented the modified Y2H assay. B.C. performed the structural analyses. B.C. and M.A.Y. performed the statistical analyses. N.S. generated the transgenic worms under the supervision of S.M. and M.B. S.M. performed survival and apoptosis challenge experiments. M.D. and V.R. performed the mutant alleles stability experiment. M.D., B.C., S.M., P.-O.V., M.E.C. and M.V. wrote the manuscript. All authors discussed the results. D.E.H. and M.V. conceived and co-directed the project.

Published online at http://www.nature.com/naturemethods/.
Reprints and permissions information is available online at http://npg.nature.com/reprintsandpermissions/.

1. Barabási, A.L. & Oltvai, Z.N. Network biology: understanding the cell's functional organization. *Nat. Rev. Genet.* **5**, 101–113 (2004).
2. Vidal, M. Interactome modeling. *FEBS Lett.* **579**, 1834–1838 (2005).
3. Shih, H.M. *et al.* A positive genetic selection for disrupting protein-protein interactions: identification of CREB mutations that prevent association with the coactivator CBP. *Proc. Natl. Acad. Sci. USA* **93**, 13896–13901 (1996).
4. Leanna, C.A. & Hannink, M. The reverse two-hybrid system: a genetic scheme for selection against specific protein/protein interactions. *Nucleic Acids Res.* **24**, 3341–3347 (1996).
5. Vidal, M., Braun, P., Chen, E., Boeke, J.D. & Harlow, E. Genetic characterization of a mammalian protein-protein interaction domain by using a yeast reverse two-hybrid system. *Proc. Natl. Acad. Sci. USA* **93**, 10321–10326 (1996).
6. Vidal, M., Brachmann, R.K., Fattaey, A., Harlow, E. & Boeke, J.D. Reverse two-hybrid and one-hybrid systems to detect dissociation of protein-protein and DNA-protein interactions. *Proc. Natl. Acad. Sci. USA* **93**, 10315–10320 (1996).
7. Endoh, H. *et al.* Integrated version of reverse two-hybrid system for the postproteomic era. *Methods Enzymol.* **350**, 525–545 (2002).
8. Gray, P.N., Busser, K.J. & Chappell, T.G. A novel approach for generating full-length, high coverage allele libraries for the analysis of protein interactions. *Mol. Cell. Proteomics* **6**, 514–526 (2007).
9. Kritikou, E.A. *et al. C. elegans* GLA-3 is a novel component of the MAP kinase MPK-1 signaling pathway required for germ cell survival. *Genes Dev.* **20**, 2279–2292 (2006).
10. Inouye, C., Dhillon, N., Durfee, T., Zambryski, P.C. & Thorner, J. Mutational analysis of STE5 in the yeast *Saccharomyces cerevisiae*: application of a differential interaction trap assay for examining protein-protein interactions. *Genetics* **147**, 479–492 (1997).
11. Serebriiskii, I., Khazak, V. & Golemis, E.A. A two-hybrid dual bait system to discriminate specificity of protein interactions. *J. Biol. Chem.* **274**, 17080–17087 (1999).
12. Hengartner, M.O., Ellis, R.E. & Horvitz, H.R. *Caenorhabditis elegans* gene *ced-9* protects cells from programmed cell death. *Nature* **356**, 494–499 (1992).
13. Yang, X., Chang, H.Y. & Baltimore, D. Essential role of CED-4 oligomerization in CED-3 activation and apoptosis. *Science* **281**, 1355–1357 (1998).
14. Conradt, B. & Horvitz, H.R. The *C. elegans* protein EGL-1 is required for programmed cell death and interacts with the Bcl-2-like protein CED-9. *Cell* **93**, 519–529 (1998).
15. del Peso, L., Gonzalez, V.M. & Nunez, G. *Caenorhabditis elegans* EGL-1 disrupts the interaction of CED-9 with CED-4 and promotes CED-3 activation. *J. Biol. Chem.* **273**, 33495–33500 (1998).
16. Yan, N. *et al.* Structure of the CED-4-CED-9 complex provides insights into programmed cell death in *Caenorhabditis elegans*. *Nature* **437**, 831–837 (2005).
17. Hengartner, M.O. & Horvitz, H.R. Activation of *C. elegans* cell death protein CED-9 by an amino-acid substitution in a domain conserved in Bcl-2. *Nature* **369**, 318–320 (1994).
18. Yan, N. *et al.* Structural, biochemical, and functional analyses of CED-9 recognition by the proapoptotic proteins EGL-1 and CED-4. *Mol. Cell* **15**, 999–1006 (2004).
19. Woo, J.S. *et al.* Unique structural features of a BCL-2 family protein CED-9 and biophysical characterization of CED-9/EGL-1 interactions. *Cell Death Differ.* **10**, 1310–1319 (2003).
20. Walhout, A.J. *et al.* Protein interaction mapping in *C. elegans* using proteins involved in vulval development. *Science* **287**, 116–122 (2000).
21. Li, S. *et al.* A map of the interactome network of the metazoan *C. elegans*. *Science* **303**, 540–543 (2004).
22. Spector, M.S., Desnoyers, S., Hoeppner, D.J. & Hengartner, M.O. Interaction between the *C. elegans* cell-death regulators CED-9 and CED-4. *Nature* **385**, 653–656 (1997).
23. Hamill, D.R., Severson, A.F., Carter, J.C. & Bowerman, B. Centrosome maturation and mitotic spindle assembly in *C. elegans* require SPD-5, a protein with multiple coiled-coil domains. *Dev. Cell* **3**, 673–684 (2002).
24. Boeke, J.D., LaCroute, F. & Fink, G.R. A positive selection for mutants lacking orotidine-5'-phosphate decarboxylase activity in yeast: 5-fluoro-orotic acid resistance. *Mol. Gen. Genet.* **197**, 345–346 (1984).
25. Rual, J.F. *et al.* Towards a proteome-scale map of the human protein-protein interaction network. *Nature* **437**, 1173–1178 (2005).
26. Lettre, G. *et al.* Genome-wide RNAi identifies p53-dependent and -independent regulators of germ cell apoptosis in *C. elegans*. *Cell Death Differ.* **11**, 1198–1203 (2004).
27. Ellis, H.M. & Horvitz, H.R. Genetic control of programmed cell death in the nematode *C. elegans*. *Cell* **44**, 817–829 (1986).
28. Boag, P.R., Nakamura, A. & Blackwell, T.K. A conserved RNA-protein complex component involved in physiological germline apoptosis regulation in *C. elegans*. *Development* **132**, 4975–4986 (2005).
29. Jeffery, C.J. Moonlighting proteins–an update. *Mol. Biosyst.* **5**, 345–350 (2009).
30. Zhong, Q. *et al.* Edgetic perturbation models of human genetic disorders. *Mol. Syst. Biol.* (in the press).
31. Venkatesan, K. *et al.* An empirical framework for binary interactome mapping. *Nat. Methods* **6**, 83–90 (2009).

ONLINE METHODS

Y2H interaction and modified Y2H. As native CED-9 is a transmembrane protein, for all Y2H and pull-down experiments we used a protein lacking the C-terminal transmembrane segment (residues 249–280), CED-9ΔTM. DB-CED-9ΔTM (wild type, L207E or W214R) was transformed into yeast cells (MaV203)[6] by standard PEG/LiAc heat shock transformation and checked for auto-activation. AD-CED-4, AD-SPD-5 or F25F8.1 were transformed in yeast cells containing DB-CED-9ΔTM. EGL-1 or CED-4 was expressed as a fusion to the SV40 nuclear localization sequence (NLS) on pMAD16 (this manuscript) a vector that carries a geneticin resistance gene for transformant selection. Co-transformants were then tested for the expression of *lacZ* and *URA3* reporter genes[32].

Quantitative β-galactosidase assay. MaV203 (ref. 6) yeast cells cotransformed with the different sets of vectors were grown overnight in selective medium (synthetic complete medium lacking leucine, tryptophan and uracil (SC-Leu-Trp-Ura) with 100 μg ml^{-1} geneticin), then diluted in fresh medium to an $OD_{600\ nm}$ of 0.1. Once cultures reached an $OD_{600\ nm}$ of 0.4–0.5, yeast cells were collected by centrifugation, then washed in 1 ml of ice-cold β-galactosidase assay buffer and lysed by adding 20 μl of chloroform and 30 μl of 10% SDS. β-galactosidase reactions were started by adding 0.8 mg of ortho-nitrophenyl-β-galactoside (ONPG; Sigma) then stopped (once a color change was observed) by adding 0.5 ml of 1 M Na_2CO_3. Reaction times were recorded. Lysates were cleared by centrifugation, then $OD_{420\ nm}$ was measured and recorded. β-galactosidase units were calculated as $1/OD_{600\ nm} \times 1{,}000/\text{time (min)} \times OD_{420\ nm}$. Units were normalized to the wild-type interaction. The Student's *t*-test was used to evaluate the significance of the difference of EGL-1 effect on CED-9(wild-type)/CED-4, CED-9(G169E)/CED-4, CED-9 (wild-type)/SPD-5 and CED-9(wild-type)/F25F8.1 comparing the β-galactosidase activity ratio in absence/presence of EGL-1.

Generation of *ced-9* alleles. The *ced-9*ΔTM ORF was mutagenized over 30 cycles of PCR using Platinum Taq HiFi DNA polymerase (Invitrogen). PCR products were cloned by Gateway reaction into pDONR-Express[8]. Full-length *ced-9*ΔTM clones were selected by plating *E. coli* on selective medium containing kanamycin and IPTG, generating about 5×10^5 transformants. All clones were scraped from plates, plasmids were isolated and their products transferred by Gateway reaction into pDEST-DB vector.

Isolation of *ced-9* edgetic alleles insensitive to EGL-1. Ten micrograms of the CED-9ΔTM mutant library were transformed by standard PEG/LiAc heat shock transformation into yeast cells (MaV203)[6] containing AD-CED-4 and EGL-1 fused to the SV40 nuclear localization sequence (NLS). Co-transformants were selected on selective medium (SC-Leu-Trp-Ura with 100 μg ml^{-1} geneticin) then tested for the expression of *lacZ* and *URA3* reporter genes[32]. *ced-9* ORFs were PCR-amplified directly from yeast colonies, sequenced then re-introduced by gap repair in fresh yeast cells containing AD-CED-4 and EGL-1, then retested. DB-CED-9 proteins recovered from the screen were also tested for auto-activation.

Yeast two-hybrid screening. DB-CED-9ΔTM was used as bait in Y2H screens against two libraries: a mixed stage cDNA library (AD-cDNA library)[33], and a normalized ORFeome library (AD-ORFeome library)[34]. Co-transformants were plated on selective medium (SC-Leu-Trp-His with 20 mM 3-aminotriazole (3AT)). AD-Y interactors were PCR-amplified directly from yeast colonies, then sequenced. From the cDNA library screen, a fragment of SPD-5 interacted with CED-9 (370 C-terminal amino acids). This fragment was used in all Y2H experiments.

Reverse Y2H selections. To carry out R-Y2H, MaV203 yeast cells were transformed with one of the AD fusion proteins and the DB-CED-9 library and then plated on selective medium (SC-Leu-Trp with 0.2% 5-fluoroorotic acid, 5-FOA). An average of 3–5 million yeast transformants were obtained for each R-Y2H screen. The 5-FOA–resistant colonies were picked and streaked onto selective medium (SC-Leu-Trp-His with 20 mM 3AT) and for β-galactosidase assays. R-Y2H alleles were PCR-amplified directly from yeast cells and PCR products were sequenced. Forward and reverse traces were aligned with wild-type *ced-9* ORF using Seqman (DNA Star package). Only single nonsynonymous missense mutants were kept for further analysis. In parallel, interactions were retested against all partners (CED-4, SPD-5 and F25F8.1)[32] and attributed a score from 0 (−) to 3 (+++), from loss of interaction to wild-type interaction.

Analysis of CED-9 mutants by western blots. GST-tagged CED-9ΔTM mutants were expressed from constructs transiently transfected into HEK293T cells. Lysates were separated on Nu-PAGE acrylamide gels (Invitrogen). After transfer to PVDF membranes, GST-tagged proteins were detected with a rabbit polyclonal antibody to GST (Sigma). Protein sample loading was controlled by probing membranes with a mouse antibody to α-tubulin (Sigma).

Validating interactions by co-affinity purification. GST–tagged CED-9ΔTM and Myc-tagged full-length partners[35] were transiently transfected into human HEK293T cells. Cleared lysates were incubated with glutathione-sepharose beads (Amersham Biosciences). Purified complexes and control lysate samples were separated on Nu-PAGE acrylamide gels (Invitrogen). After transfer to PVDF membranes, Myc and GST-tagged proteins were detected with a mouse monoclonal antibody to Myc (clone 9E10) and a rabbit polyclonal antibody to GST (Sigma). Co-AP results were scored from 0 (–) to 3 (+++), from complete loss-of-interaction to wild-type.

CED-9 structures. Three CED-9 X-ray crystallographic structures have been solved to date: CED-9 alone (PDB identifier: 1OHU)[19], CED-9 in complex with the EGL-1 BH3 peptide (PDB ID code 1TY4)[18], and CED-9 in complex with a CED-4 dimer (PDB: 2A5Y)[16]. As these structures differ in the amino acids missing at the N and C termini, amino acids that were not present in all three structures were discarded to allow comparison between these structures. The common region used was Glu75–Arg237. The structures were fitted to the wild-type CED-9 sequence. For the CED-9 and the CED-9/EGL-1 structures, selenomethionine were replaced by methionine. For the CED-9 and the CED-9/CED-4 structures, serine residues at positions 107, 135, and 164 were replaced by the original cysteine residues. The CED-9/EGL-1 structure contains a L148P substitution. This proline was replaced

doi:10.1038/nmeth.1394

by a leucine using Modeller[36]. Modeller was also used to add the missing Thr161 and Asp162 in the CED-9/CED-4 structure and missing side chains. All tertiary structures were optimized with HyperChem (release 6.1 for Windows Hypercube) by a conjugated gradient procedure using the AMBER96 force field until reaching an RMS gradient lower than 0.01 kcal $Å^{-1}$ mol^{-1}. Figures of tertiary structures were generated with PyMol.

Analysis of surface exposure of edgetic/non-edgetic residues. The relative solvent-accessible surface areas (ASAs) were calculated for the three CED-9 structures as described previously[37]. Residues were called accessible if their ASA was above 10% in at least one of the three structures, or buried if below this threshold in all three structures. This criterion was chosen to take into account variations between the three available CED-9 structures. The analysis was then repeated using ASA cutoffs of 20 and 30%.

For the same reason, statistical tests were carried out for each residue using the maximal ASA observed in the three CED-9 structures. The maximal ASA values of the 19 partner-specific edgetic residues were averaged and compared to the value obtained with 1,000,000 sets of 19 residues picked at random in CED-9. Picking the same residue several times for the same set was prohibited because edgetic alleles isolated several times were only counted once. Similar tests were done with random sets of 16 and 23 residues for the edgetic alleles defective for two interactions and for the non-edgetic alleles, respectively. The observed average maximal ASA was then compared to the distribution of the average of the random sets to determine the statistical significance by empirical *P*-value. Randomizations done with the three structures independently or with the average ASA of the three structures gave similar results.

Trp73 (in protein encoded by SPD-5-specific edgetic allele) and Glu241 (in protein encoded by non-edgetic allele) residues were not included in the ASA analysis because they are not present in all three structures. When alleles were mutated at the same position but with distinct substitutions having different interaction profiles (for example, CED-9(G82E) and CED-9(G82R), which are defective for SPD-5 only and for both CED-4 and SPD-5, respectively), the corresponding residue was included in both sets (one or two interaction–defective edgetic alleles in our example).

Analysis of CED-9/CED-4 interactions in the co-crystal structure. The CED-9/CED-4 interface was analyzed on the co-crystal structure after the addition of hydrogen atoms with PyMol. The non-edgetic Glu241 residue was included because it is present in the tertiary structure. When alleles were mutated at the same position but with distinct substitutions having different interaction profiles (for example, CED-9(P106Q) and CED-9(P106R), which are defective for CED-4 only and for both CED-4 and SPD-5, respectively), the corresponding residue was included in both sets (one- or two-interaction defective edgetic alleles in our example).

CED-9 residues at the CED-9/CED-4 interface were detected using a distance cutoff of 4.0 Å. At this cutoff, 41 of 175 CED-9 residues are in contact with CED-4. *P*-values were calculated by the hypergeometric test. We calculated the probability of having 6/6, at least 7/14, or maximum 1/24 residues at the interface, for the set of residues defective for CED-4 only, for CED-4 and another partner, and for all three partners, respectively.

For each residue of CED-9, the minimal distance to CED-4 was calculated as the distance between the two closest atoms. For each set of residues (residues defective for CED-4 only, for CED-4 and another partner, and for all three partners), the average distance to CED-4 was calculated and compared to the average obtained for 1,000,000 sets of 6, 14 or 24 residues, respectively, picked at random in CED-9. Picking the same residue several times for the same set was prohibited. Empirical *P*-values were calculated via the comparison of the observed average to the distribution of the random sets.

***C. elegans* strains.** Methods for growing *C. elegans* were described previously[38]. All strains were grown at 20 °C, maintained on NGM medium on op50 bacteria, HB101 bacteria for growth in liquid culture or on HT115 bacteria for RNAi experiments. The following worm strains were used: Bristol strain N2, MT5523 (*unc-69(e587) ced-9(n1950n2161)*/qCi *dpy-19(e1259) glp-1(q339)* III); MT1522 (*ced-3(n717)*IV); DP38 (*unc-119(ed3)*III); wild-type transgene, CED-9(K207E), CED-9(W214R).

Generation of transgenic *C. elegans* strains. A 4 kb genomic DNA fragment containing the *ced-9* operon (consisting of *cyt-1* and *ced-9*) and 400 bp of upstream and 600 bp of downstream flanking sequences was cloned from N2 genomic DNA, then cloned by Gateway reaction into pDONR223. Mutations were introduced in the 4 kb genomic DNA fragment with the Gene Tailor site-directed mutagenesis (SDM) kit (Invitrogen). Mismatched primers were designed according to the manufacturer's protocol. The full-length *ced-9* gene was sequenced from the SDM products to ensure that only the intended mutation was present and that the sequence was otherwise wild-type. The correct SDM product was cloned by Gateway reaction into pID2.02. Transgenic lines were generated by microparticle bombardment[39]. Homozygous transgenic worms were crossed into MT5523. Homozygous transgenic worms carrying the transgene were confirmed by PCR-amplification of *ced-9* and flanking vector specific sequences. The presence of the closely linked *unc-69*(*e587*) marker was used to assess the presence of *ced-9*(*n1950n2161*). Genotypes of all crosses were confirmed by sequencing.

MT5523 (*unc-69*(*e587*) *ced-9*(*n1950n2161*)) was used as a negative control to compare the magnitude of the survival rate in transgenic worm strains. Number of embryos laid and survival rate were measured as before[40]. P_0 worms that died within the first 2 d of the experiment were not analyzed. To evaluate the significance of both average number of embryos laid and the corresponding survival rate, we calculated the significance of differences compared to *ced-9* null allele worms (*ced-9(n1950n2161)*) expressing wild-type *ced-9*, using a Student *t*-test for the average number of embryos laid and a binomial distribution test for the corresponding survival rate.

RNAi clones of *ced-4* and *cpb*-3 came from the *C. elegans* ORFeome-RNAi v1.1 library[41]. As a *ced-9* RNAi clone was unavailable, this clone was transferred from an Entry clone (*C. elegans* ORFeome v1.0 library)[34] into pL4440-DEST-RNAi. RNAi on plates was carried out as described[42]. RNAi in liquid medium was essentially performed as described previously[43]. Apoptotic germ cell corpses were identified and quantified

based on their characteristic morphology under differential interference contrast (DIC) microscopy, or using SYTO-12 (Molecular Probes), as described previously[44].

32. Walhout, A.J. & Vidal, M. High-throughput yeast two-hybrid assays for large-scale protein interaction mapping. *Methods* **24**, 297–306 (2001).
33. Walhout, A.J. *et al.* GATEWAY recombinational cloning: application to the cloning of large numbers of open reading frames or ORFeomes. *Methods Enzymol.* **328**, 575–592 (2000).
34. Reboul, J. *et al. C. elegans* ORFeome version 1.1: experimental verification of the genome annotation and resource for proteome-scale protein expression. *Nat. Genet.* **34**, 35–41 (2003).
35. Xu, L. *et al.* BTB proteins are substrate-specific adaptors in an SCF-like modular ubiquitin ligase containing CUL-3. *Nature* **425**, 316–321 (2003).
36. Sali, A. & Blundell, T.L. Comparative protein modelling by satisfaction of spatial restraints. *J. Mol. Biol.* **234**, 779–815 (1993).
37. Lins, L., Thomas, A. & Brasseur, R. Analysis of accessible surface of residues in proteins. *Protein Sci.* **12**, 1406–1417 (2003).
38. Brenner, S. The genetics of *Caenorhabditis elegans*. *Genetics* **77**, 71–94 (1974).
39. Praitis, V., Casey, E., Collar, D. & Austin, J. Creation of low-copy integrated transgenic lines in *Caenorhabditis elegans*. *Genetics* **157**, 1217–1226 (2001).
40. Hofmann, E.R. *et al. Caenorhabditis elegans* HUS-1 is a DNA damage checkpoint protein required for genome stability and EGL-1-mediated apoptosis. *Curr. Biol.* **12**, 1908–1918 (2002).
41. Rual, J.F. *et al.* Toward improving *Caenorhabditis elegans* phenome mapping with an ORFeome-based RNAi library. *Genome Res.* **14**, 2162–2168 (2004).
42. Timmons, L., Court, D.L. & Fire, A. Ingestion of bacterially expressed dsRNAs can produce specific and potent genetic interference in *Caenorhabditis elegans*. *Gene* **263**, 103–112 (2001).
43. Lehner, B., Tischler, J. & Fraser, A.G. RNAi screens in *Caenorhabditis elegans* in a 96-well liquid format and their application to the systematic identification of genetic interactions. *Nat. Protocols* **1**, 1617–1620 (2006).
44. Gumienny, T.L., Lambie, E., Hartwieg, E., Horvitz, H.R. & Hengartner, M.O. Genetic control of programmed cell death in the *Caenorhabditis elegans* hermaphrodite germline. *Development* **126**, 1011–1022 (1999).

doi:10.1038/nmeth.1394

Erratum: 'Edgetic' perturbation of a *C. elegans* BCL2 ortholog

Matija Dreze, Benoit Charloteaux, Stuart Milstein, Pierre-Olivier Vidalain, Muhammed A Yildirim, Quan Zhong, Nenad Svrzikapa, Viviana Romero, Géraldine Laloux, Robert Brasseur, Jean Vandenhaute, Mike Boxem, Michael E Cusick, David E Hill & Marc Vidal
Nat. Methods **6, 843–849 (2009); published online 25 October, 2009; corrected after print 16 November 2009.**

In the version of this article initially published, the schematic in Figure 5a was misaligned. The error has been corrected in the HTML and PDF versions of the article.